Available online at www.sciencedirect.com

ScienceDirect

Procedia Engineering 109 (2015) 17 – 26

Procedia Engineering

www.elsevier.com/locate/procedia

XXIII Italian Group of Fracture Meeting, IGFXXIII

Numerical modeling of aluminum alloys fracture for automotive applications

Luca Cavazzoni[a], Giuseppe Miscia[a], Vincenzo Rotondella[a], Andrea Baldini[a]*

[a]*Department of Engineering "Enzo Ferrari", University of Modena and Reggio Emilia, Via P. Vivarelli 10, Modena, 41125, Italy*

Abstract

Nowadays, finite element analysis assumes a key-role in the automotive industry. Predictivity of FE models has been strongly improved during the last years and the research on this topic involves both industrial and academic fields. The main focus of this paper is the prediction of the failure of aluminum alloys used for extruded components. Material fracture affects the capacity of absorbing energy and the crashworthiness of the structure as well. In extracting the samples directly from the components involved in the crash event, it has been possible to take into account the whole manufacturing process. The methodology has been developed to improve the correlation of the FE models as well as to answer to the industrial requirements.

Peer-review under responsibility of the Gruppo Italiano Frattura (IGF)

Keywords: Experimental-numerical correlation, Failure model, Aluminum alloys, FEA, Crashworthiness;

Nomenclature

σ , σ_{true} , σ_{eng}	Stress, true stress, engineering stress
ε , ε_{true} , ε_{eng}	Strain, true strain, engineering strain
σ_{ij}	Cauchy stress tensor
σ_{VM}	Von Mises stress
σ_H	Hydrostatic mean stress

* Prof. Andrea Baldini. Tel.: +39-059-2056280.
E-mail address: millechililab@unimore.it

Peer-review under responsibility of the Gruppo Italiano Frattura (IGF)
doi:10.1016/j.proeng.2015.06.203

F , G , H , L , M , N , R	Hill's material constants
σ_{Heq}	Hill's equivalent stress
A_{ij}	Hill's constants in plane stress state
r_{00} , r_{45} , r_{90}	Lankford's parameters
σ_{eq}	Stress triaxiality
ε_f	Equivalent strain to failure
D_1, D_2 , D_3	Johnson-Cook material constants
a , b	Bao-Wierzbicki material constants

1. Introduction

The international safety standards require several kinds of experimental tests in order to validate the performances of a vehicle under crash loads. The chassis is widely involved during an accident and for this reason it is important to investigate the crashworthiness of the structure. Aluminum is a common material used to design vehicle chassis thanks to its physical and mechanical properties. The capability of absorbing energy strongly depends on the possibility of fracture occurrence in the material. For this reason, the predictivity of FE analysis becomes relevant in order to design and validate a structure before the experimental tests. Fracture prediction in metal materials has been widely studied and several criteria have been defined and compared in the literature [1-4]. Accuracy, complexity, number and cost of the experimental tests are parameters that vary depending on the failure criteria studied.

In order to achieve a better prediction the material behavior in the FEA, the experimental phase is based on the extraction of samples directly from the components involved during the crash test. In this way, it is possible to include all the manufacturing process effects. Due to the limited areas available on the components, only tensile [5] and shear [6] specimens have been considered in the presented study. The fracture prediction for compression and mixing stress-strain states has been supposed using the analytical functions provided by the failure criteria chosen. As it will be shown in the paper, different formulations have been used to define the fracture locus of the alloys studied. It is possible to suppose the manufacturing process could affect the material properties more than expected: the samples extraction phase from the components allows for the consideration of any residual plastic strains into the material. Furthermore, the extrusion process may cause an anisotropy effect into the material. A specific material card included in Altair Radioss explicit code has been tuned to define the anisotropy of the material [7].

This work represents the initialization of a wide activity dealing with the FE models predictivity. For a first approach, the side pole crash has been considered as test case. The door sills, the tunnel and the rear sills transverse are the main components involved during this test and for this reason they have been used for the specimens extraction. It is necessary to specify that this methodology may be adopted for different cases: casting and laminated components may be assessed as well. In particular, for casting components, it is enough to set isotropic parameters in the material card.

2. Methods and results

The side pole crash has been used as test case for a first approach. The aluminum alloys studied come from the main chassis components involved during the test: 6005T6 (door sills), 6063T6 (bottom sills transverse and tunnel), 6181AT6 (top sills transverse), as shown in Fig. 1. The specimens have been directly extracted from the components depending on the space availability (as represented in Fig. 2). Since they have been obtained by the extrusion manufacturing process, tensile 0°-45° and 90° have been cut in order to evaluate the anisotropy, see Fig.3. In the case in which it was not possible to extract tensile 45° and 90° as well, any anisotropy investigation has been done and an isotropic material card has been defined.

ASTM B557-02a [5] and ASTM B831-93 [6] have been followed for the specimens extraction. Due to the limited transversal size of the components, only the 0° specimens respect the dimension suggested by the standards. In order to use the tensile testing machine for both the tensile and the shear tests the shear specimens dimensions follow the standard. From the Force–Displacement curve of the tensile 0° test, the Engineering Stress-Strain curve has been calculated. Fig. 4 shows the wide dispersion of the experimental results of the tensile 0° tests. Cutting the specimens from different faces and position of the extruded part, it is possible to observe how the manufacturing process may differently affect the material characteristics.

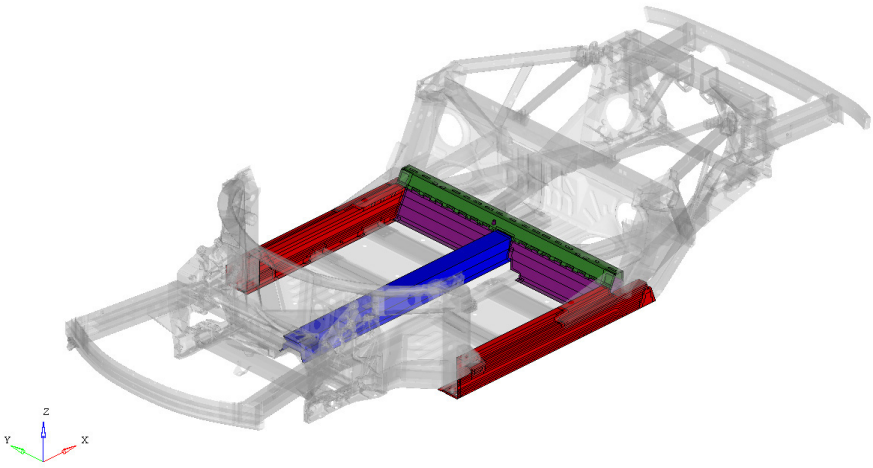

Fig. 1. 6005T6 (door sills) in red, 6063T6 (bottom sills transverse) in violet, 6063T6 (tunnel) in blue, 6181AT6 (top sills transverse) in green.

Fig. 2. Extraction of the specimens from the chassis components.

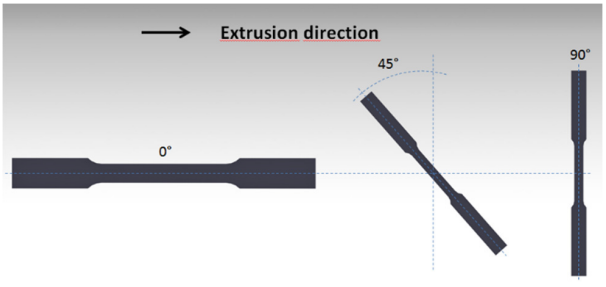

Fig. 3. Tensile 0°-45°-90° specimens.

These curves do not take into account the real trend of the stress during the necking phase. Therefore, Eq. 1-2 have been used to estimate the True Stress-Strain curve of the tensile 0° test up to the maximum force (corresponding to the necking point).

$$\sigma_{true} = \sigma\left(1+\varepsilon_{eng}\right) \tag{1}$$

$$\varepsilon_{true} = ln\left(1+\varepsilon_{eng}\right) \tag{2}$$

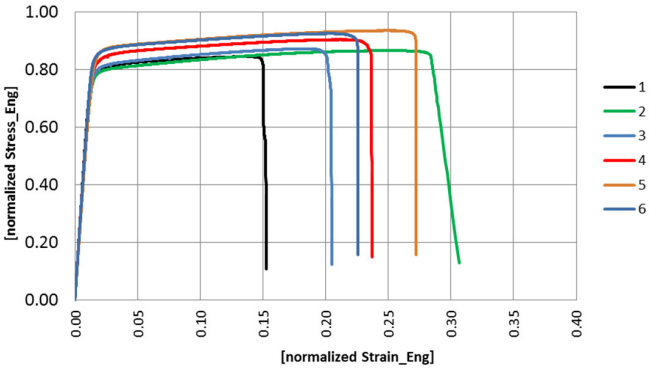

Fig. 4. Engineering Stress-Strain curve of 6005T6 specimens. Normalized curves are obtained dividing each original curve by a constant.

The necking point has been determined according to Eq.3

$$\frac{d\sigma_{true}}{d\varepsilon_{true}} = \sigma_{true} \tag{3}$$

After the necking point, the true $\sigma-\varepsilon$ trend has been estimated using a FEA iterative process. Fig. 5 shows the limits used to define this trend: the lower bound limit defined by a null slope and the upper bound limit defined by the last slope of the curve before the necking point. The correlation has been carried on using a 0.2mm mesh size for the FE models. In fact, it is important to accurately read the stress and the strain in the material. A study of the mesh size effect is proposed at the end of the chapter. The experimental Force – Displacement curve has been fitted supposing the trend of the true stress-strain curve in the Radioss material card. To respect the physical behavior of the metal, an increasing trend must be used. Fig. 5 shows the 6063T6 correlation using for example only two points (hence, two straight lines with increasing slope).

The true stress-strain curve of the tensile 0° test has been used to set the Hill's law [7] (Radioss LAW 43). Hill defined for the anisotropic behavior a yield surface as following:

$$\left(\sigma_{22}-\sigma_{33}\right)^2 + G\left(\sigma_{33}-\sigma_{11}\right)^2 + H\left(\sigma_{11}-\sigma_{22}\right)^2 + +2L\sigma_{23}^2 + 2M\sigma_{31}^2 + 2N\sigma_{12}^2 - 1 = 0 \tag{4}$$

F, G, H, L, M, N are the material constants and the stress σ_{IJ} are expressed in the Cartesian reference parallel to the three planes of anisotropy. Eq. 4 can be simplified using the assumption of plane stress:

$$\sigma_{Heq} = \sqrt{A_1\sigma_{11}^2 + A_2\sigma_{22}^2 - A_3\sigma_{11}\sigma_{22} + A_{12}\sigma_{11}^2} \tag{5}$$

The coefficients A_i are determined using Lankford's anisotropy parameter r_α :

$$A_1 = H\left(1+\frac{1}{r_{00}}\right);\ A_2 = H\left(1+\frac{1}{r_{90}}\right);\ A_3 = 2H \tag{6}$$

$$A_{12} = 2H\left(r_{45}+0.5\right)\left(\frac{1}{r_{00}}+\frac{1}{r_{90}}\right);\ H = \frac{R}{1+R};\ R = \frac{r_{00}+2r_{45}+r_{90}}{4}$$

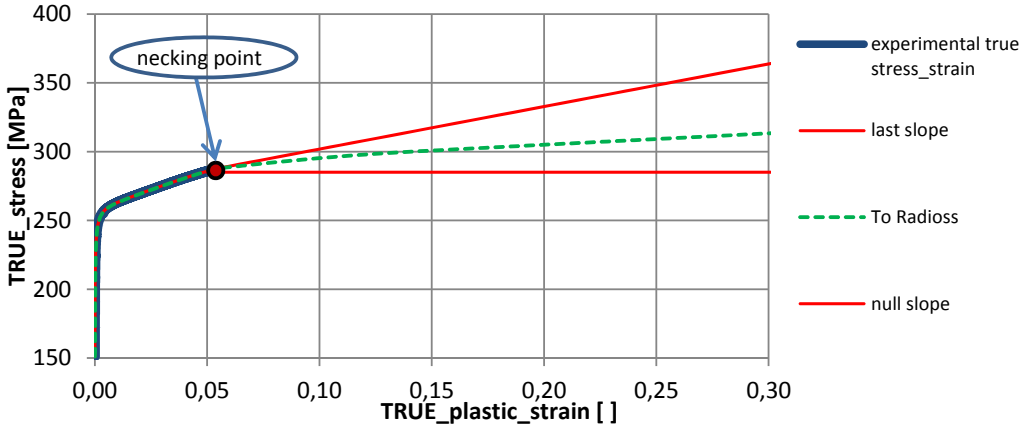

Fig. 5. Definition of the post-necking trend of the Radioss material card.

The Lankford parameters can be set in order to obtain the specimen correlation in terms of loads. In fact, Hill's criterion does not consider the anisotropy effects on the strain. The Lankford parameters defined for the material studied are listed in Tab.1. As shown, for the 6181AT6 the isotropic condition has been set: no specimens in 45° and 90° were cut due to the limited space available on the component.

Due to the complexity of Eq. 4, a Design-Of-Experiments has been performed to support the Force-Displacement fitting. DoE allows the sample of the design domain and also the estimation of the influence and interactions of the variables on the controlled responses. A full factorial method has been used imposing the coefficients A_i as variables and the Lankford parameters as responses. This preliminary screening has been useful to determine a reliable set of solution in terms of material coefficients A_i. Fig. 6 shows the results of the 6063T6 after tuning the Hill's material card. It is possible to notice the slopes in tensile 45°-90° and shear are different between numerical and experimental. This is due to a lack of a suitable extensometer during the experimental tests for this kind of specimens. However, the failure criteria used do not consider the anisotropy effect. Hence, the equivalent strain to failure in tensile 0° affects the 45° and 90° cases as well (the correlation in terms of displacements is not required). Further hypothesis for the displacements correlation are explained in the next parts of the paper.

Table 1. Lankford parameters for 6063T6 , 6005T6 and 6181AT6

	r_{00}	r_{45}	r_{90}
6063T6	1	0.98	0.85
6005T6	0.83	0.94	0.72
6181AT6	1	1	1

The following phase deals with the fitting of the load drop. A failure card has been added to consider the shell elements deleting, according to the fracture criteria. In this work two different failure models have been considered: Bao-Wierzbicki [8] and Johnson-Cook [9] failure models. These criteria define the trend of the equivalent strain to failure depending on the stress triaxiality:

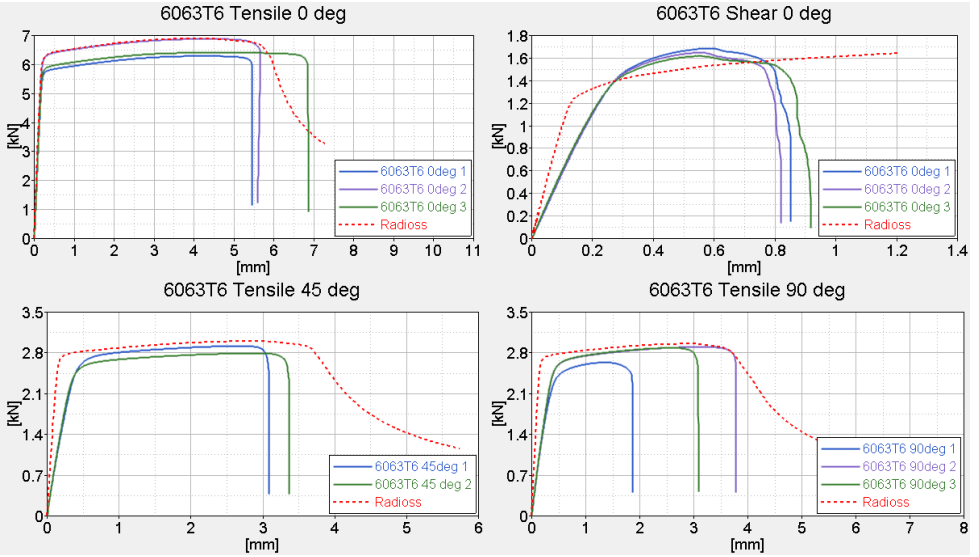

Fig. 6. Results of the 6063T6 after tuning the Hill's material card.

$$\varepsilon_f = \left[D_1 + D_2 exp\left(D_3 \sigma_{eq} \right) \right] \tag{7}$$

$$\varepsilon_f = \begin{cases} \infty & \sigma_{eq} \le \frac{1}{3} \\ \frac{a}{1+3\sigma_{eq}} & -\frac{1}{3} < \sigma_{eq} \le 0 \\ 9\left(b-a\right)\sigma_{eq}^2 + a & 0 \le \sigma_{eq} \le \frac{1}{3} \\ \frac{b}{3\sigma_{eq}} & \frac{1}{3} \le \sigma_{eq} \le \frac{2}{3} \end{cases} \quad ; \quad \sigma_{eq} = \frac{\frac{\sigma_I + \sigma_{II} + \sigma_{III}}{3}}{\sigma_{VM}} \tag{8}$$

where σ_I, σ_{II}, and σ_{III} are the principal stress and σ_{VM} is the Von Mises stress. D_1, D_2, D_3, a, b are the material constants. In the J-C equation, no temperature and strain rate effect have been considered.

The maximum displacements reached during the experimental tests have been used to define the equivalent strain to failure of the fracture models: running the FE models of tensile 0° and shear without a failure card, it is possible to read the elements equivalent strains at the instant when the load drop should occur. This strain value has been used to define the failure strain tuning the J-C and B-W constants. The choice of the failure model has been made depending on the failure limits defined. In fact, J-C model shows a decreasing trend of the equivalent strain to fracture, while B-W is represented by higher limit in tensile than in shear. Concerning the compression limit, the trend has been supposed providing very high values of strain limits.

- $\varepsilon_{f\_tensile} < \varepsilon_{f\_shear}$ → J-C failure model (Fig. 7).
- $\varepsilon_{f\_tensile} > \varepsilon_{f\_shear}$ → B-W failure model (Fig. 8).

In the following pictures (Fig. 9-10) it is possible to observe the stress triaxiality and the equivalent strain to

failure in the FE samples. On the left is shown the run without failure card: no ruptures occur and the equivalent strain to failure has been extracted according to the experimental data. The pictures also show the differences in terms of failure (on the right). In the 6063T6 shear sample, the crack formation occurs close to the edge of the central section (high triaxiality state). In fact, using a JC model, the tensile strain to failure is lower than the shear one.

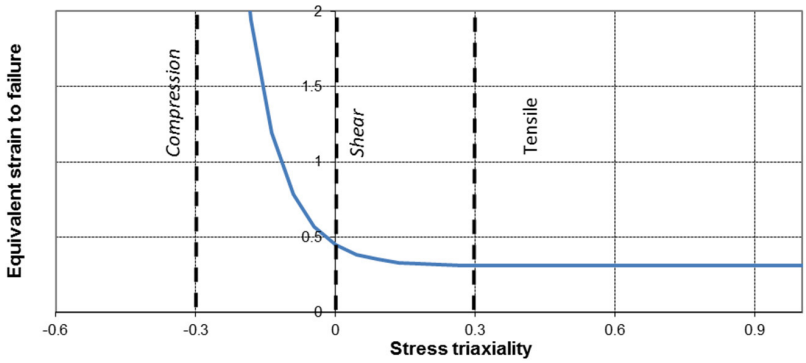

Fig. 7. 6063T6 J-C failure model.

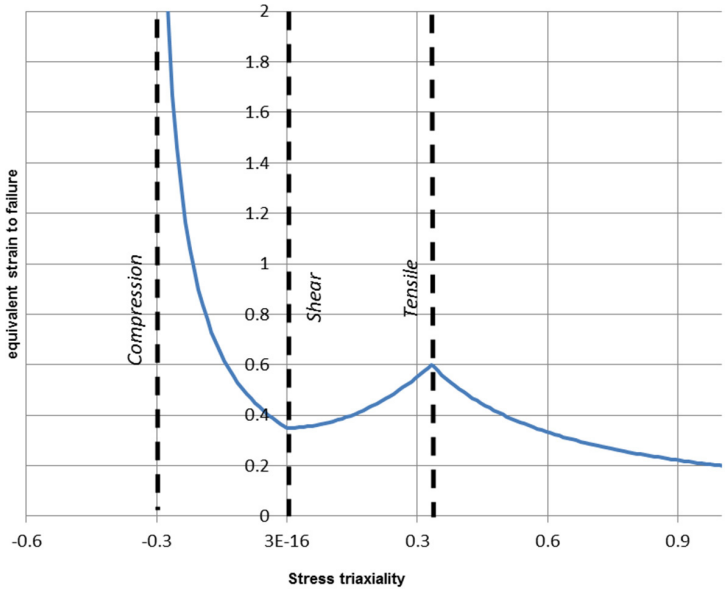

Fig. 8. 6005T6 B-W failure model.

The numerical Force-Displacement curves have been compared with the experimental ones. For instance, Fig. 11 shows the comparison for the 6005T6 alloy. In the case of the tensile 0° tests, only one curve was taken as reference for the correlation due to the different thicknesses of the samples tested. The load and the maximum displacements are well predicted. Concerning the tensile 45° and 90° cases, only the load can be fitted (as explained before the fracture criteria does not consider the anisotropy effect). The comparison of the shear test shows differences in terms of both forces and displacements. In particular, the forces have been underestimated and the maximum displacement has been overestimated. Since the extensometer was not suitable on the shear samples, the measurements have been

directly performed by the cross-bar of the tensile machine (this explains the stiffness difference in the first part of the curve).

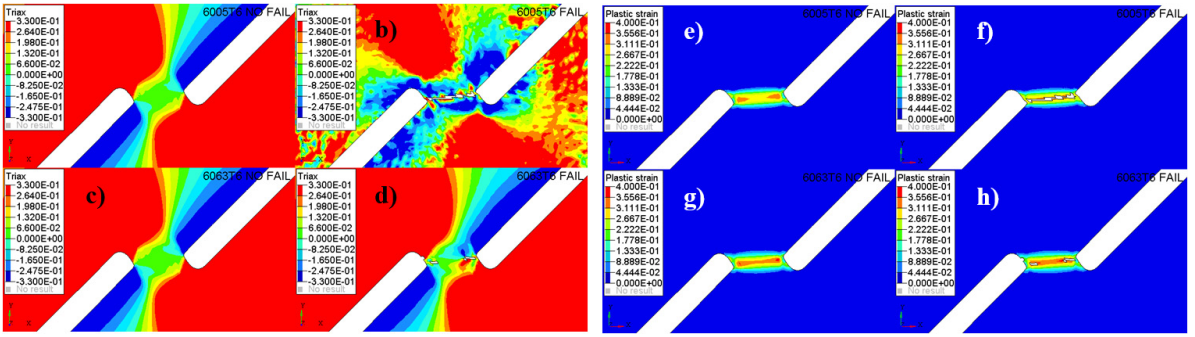

Fig. 9. (left) Triaxiality stress in the shear tests: a) 6005T6 without failure, b) 6005T6 with failure, c) 6063T6 without failure, d) 6063T6 with failure; (right) Equivalent strain in the shear tests : e) 6005T6 without failure, f) 6005T6 with failure, g) 6063T6 without failure, h) 6063T6 with failure.

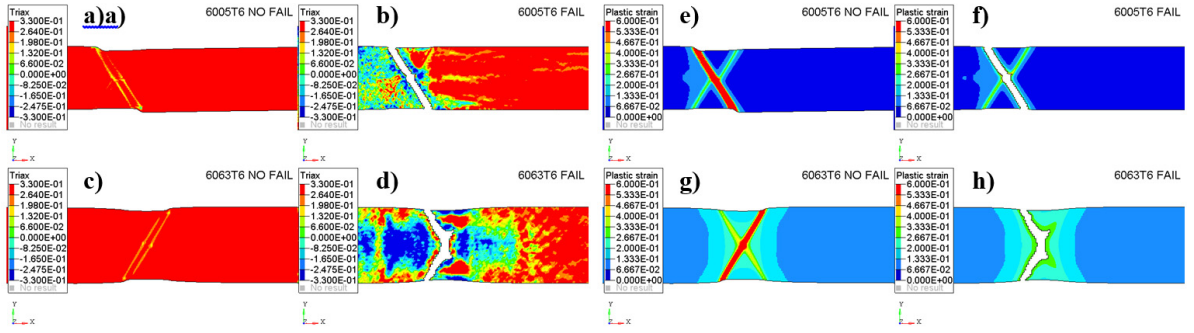

Fig. 10. (left) Triaxiality stress in the tensile tests: a) 6005T6 without failure, b) 6005T6 with failure, c) 6063T6 without failure, d) 6063T6 with failure; (right) Equivalent strain in the tensile tests: e) 6005T6 without failure, f) 6005T6 with failure, g) 6063T6 without failure, h) 6063T6 with failure.

As already mentioned, a 0.2mm mesh-size has been used in the initial correlation to better calculate the stress and strain values in FEA. In a full vehicle model a coarse mesh-size is needed to reduce the computational time (5-10mm). To obtain coherent results between a 0.2 mm and a 10 mm mesh-sizes model, it is necessary to define a mesh scaling function. The scaling factor directly affects the failure function (the greater is the mesh size and the lower is the scaling factor). The tensile 0° specimen has been modeled with different mesh sizes. In Fig. 12 is shown the mesh scaling function of the 6005T6 alloy. In general, it varies depending on the material studied.

3. Conclusions

This paper aims at defining a methodology in order to predict the aluminum failure in automotive crash applications. The activity has been developed in collaboration with Ferrari S.p.a. and it is a preliminary phase of a wide project that aims at refining the FE models used in crash analysis.

Predictivity in the failure of the aluminum alloys usually requires a huge and detailed experimental campaign. The present work tries to provide a simplified methodology based on a limited number of experimental tests. In extracting the specimen directly from the final components, it is possible to consider the manufacturing effect during the correlations. It has been also noticed that extruded components made by the same aluminum alloy but subjected

to different extrusion matrix show different mechanical properties. Therefore, during the numerical correlation, it could be necessary to define a specific material card for each component and not only for the aluminum alloy class.

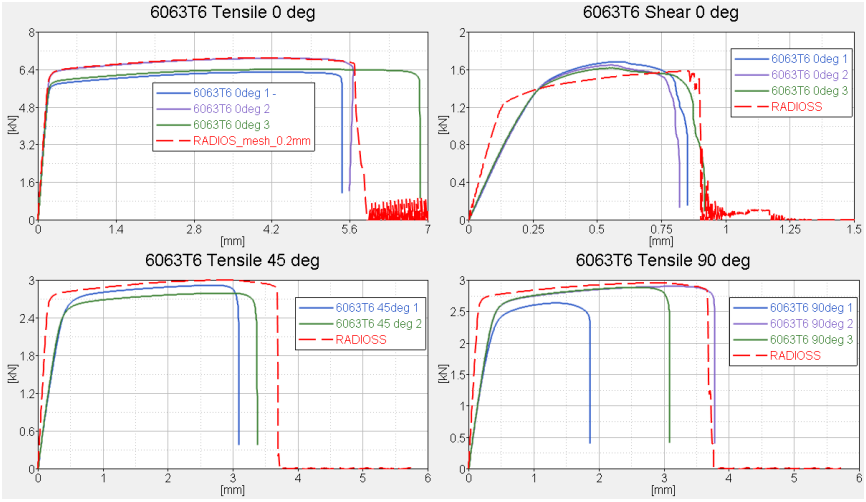

Fig. 11. Correlation results of 6005T6 alloy

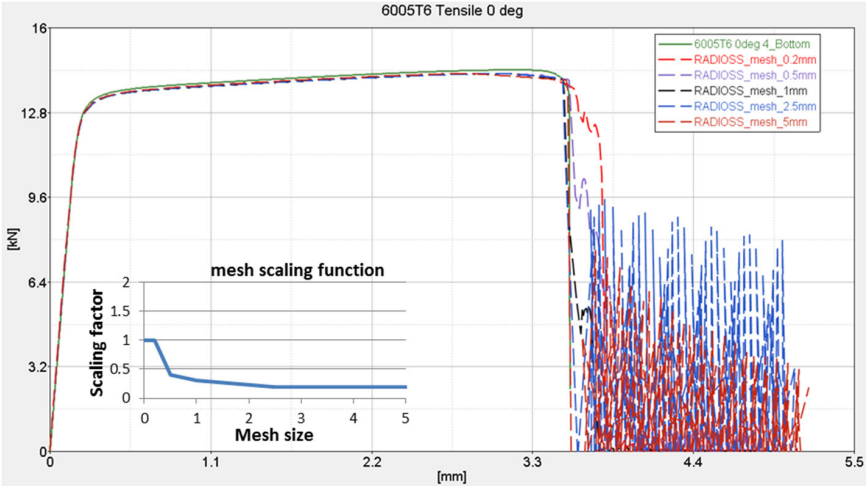

Fig. 12. Definition of the mesh scaling function on the tensile 0° test

Due to the limited dimensions of the chassis components, only two kinds of test have been taken into account. Uniaxial tensile test and shear test have been performed in order to determinate the equivalent strain to failure. Depending on the test results, a failure criterion has been chosen to define the fracture locus curve. Using the J-C and the B-W equations, it has been possible to suppose the whole fracture locus plane: mixing state limits have been determined following the trend of the functions given by the failure criteria and the compression limit has been hypothesized. By cutting uniaxial specimens in 0°, 45° and 90°, it has been possible to include the anisotropy of the material in the FE analysis as well.

The FE analyses on samples have been performed with a mesh size of 0.2 mm and J-C and B-W failure criteria have been numerically validated. Both criteria are potentially convenient for numerical simulation in automotive

field also because they are integrated in the most of the explicit solvers. The suggested methodology, thanks to a definition of a mesh scaling function, is mesh-size-independent and it could be applied to the Full-Vehicle models that usually present a medium mesh size greater than 5 mm. The mesh size effect has been evaluated on the tensile 0° test. However, an intermediate phase between the samples correlation and the Full-Vehicle validation could be necessary: the validation of the mesh-scaling function on a single component allows a further investigation on it.

The methodology can be extended also to other class of part of the chassis. Plates usually show anisotropy due to the laminating process. Furthermore, moving to an isotropic material card it is possible to study the correlation of castings. Future developments deal with the modeling of the residual plastic strain after manufacturing and the automatization of the correlation process by using optimization techniques.

Acknowledgements

Acknowledgments to Ferrari S.p.a. and in particular to Eng. Andrea Merulla and Eng. Luca D'Agostino for supporting the research activity.

References

[1] A.G. Atkins, Fracture mechanics and metalforming: damage mechanics and the local approach of yesterday and today, H.P. Rossmanith (Ed.), Fracture Research in Retrospect, An Anniversary Volume in Honour of George R. Irwin's 90th Birthday, A.A. Balkema, Rotterdam, Brookfield, (1997), pp. 327–352

[2] F.A. McClintock, Slip line fracture mechanics: A new regime of fracture mechanics. Fatigue and Fracture Mechanics, ASTM STP-1417, West Conshohocken, PA. 33 (2002).

[3] T. Wierzbicki, Y. Bao, Y.W. Lee, Y. Bai, Calibration and evaluation of seven fracture models, Int. J. Mech. Sci. 47 (2005) 719–743

[4] Y. Bai, Effect of Loading History on Necking and Fracture, Massachusetts Institute of Technology, PhD thesis, 2008.

[5] ASTM B557-02a, Standard Test Methods of Tension Testing Wrought and Cast Aluminum- and Magnesium-Alloy Products, ASTM International, West Conshohocken, PA, 2002.

[6] ASTM B831-93, Standard Test Method for Shear Testing of Thin Aluminum Alloy Products, ASTM International, West Conshohocken, PA, 1998.

[7] Altair Engineering, Inc., Altair HyperWorks 13 - RADIOSS User's Guide, Troy, Michigan, USA.

[8] G. R. Johnson, W. H. Cook, Fracture characteristics of three metals subjected to various strains, strain rates, temperatures and pressures, Engineering Fracture Mechanics. 21(1) (1985) 31-48.

[9] Y.W. Lee, Fracture Prediction in Metal Sheets, Massachusetts Institute of Technology, PhD thesis, 2005.